Chinese Journal of Chemical Engineering 76 (2024) 272–280

Contents lists available at ScienceDirect

Chinese Journal of Chemical Engineering

journal homepage: www.elsevier.com/locate/CJChE

Full Length Article

Preparation of coconut oil/aluminum nitride/expanded graphite composite phase change materials with high thermal conductivity and stable shape for thermal energy storage

Chao Gao [1,*], Feng Jiang [2], Benguo Zhang [2], Mingchuan Shen [2], Yuguo Zhang [2]

[1] School of Mechanical Engineering, Changshu Institute of Technology, Suzhou 215500, China
[2] School of Mechanical Engineering, Yancheng Institute of Technology, Yancheng 224051, China

ARTICLE INFO

Article history:
Received 18 June 2024
Received in revised form
7 August 2024
Accepted 19 August 2024
Available online 21 September 2024

Keywords:
Energy material
Thermal energy storage
Phase change material

ABSTRACT

Phase change energy storage is one of the solutions to effectively deal with the problem of intermittency and spatial and temporal mismatch between supply and demand of new energy sources (solar, wind, *etc.*). However, phase change materials (PCMs) suffer from low thermal conductivity, which greatly affects energy storage and release efficiency. In this study, a novel shape-stable phase change material (SSPCM) was prepared by mixing coconut oil (CO) as a PCM with aluminum nitride (AlN) thermally conductive reinforcing particles and vacuum impregnated into expanded graphite (EG). The results showed that the thermal conductivity of the prepared SSPCM reached 2.985 $W \cdot m^{-1} \cdot K^{-1}$, which was 1765% higher than that of pure CO. The latent heat of SSPCM was 83.67 $J \cdot g^{-1}$, which was 99% of the theoretical value. Furthermore, SSPCM showed excellent thermal stability and thermal cycle reliability. The proposed SSPCMs have the advantages of being renewable and simple preparation methods, which have great potential for application.

1. Introduction

Energy issues have always been emphasized by people, fossil energy will be exhausted one day, and the environmental problems such as the greenhouse effect are increasing in the process [1,2]. Finding renewable and environmentally friendly new energy sources to replace fossil energy has become urgent [3]. Solar, wind, and geothermal energy are considered to be very promising new energy sources. However, they have disadvantages such as volatility and intermittency, which make it difficult to apply them [4,5].

Combining new energy storage technologies with new energy sources is one of the means to effectively solve these problems [6]. Thermal energy storage (TES) system stands out with its advantages of low cost and long service life. TES can be categorized into sensible heat TES, latent heat TES, and thermochemical heat TES [1]. Compared with the other two TES methods, latent heat TES based on phase change materials (PCM) has a higher energy storage density while storing and releasing heat with less temperature change, more stability and reliability, and fewer equipment requirements [7,8]. These features make it play an important role in the fields of waste heat recovery [9], battery thermal management [10], and building energy efficiency [11,12].

PCM can be divided into organic PCM and inorganic PCM according to its chemical composition. Generally speaking, inorganic PCM has a higher enthalpy of phase change and is cheaper, but there is a subcooling phenomenon, easy to phase separation, and corrosive. Organic PCMs have little or no subcooling during crystallization and are generally non-corrosive. However, conventional PCMs, especially organic PCMs, face two great challenges: thermal conductivity is too low and they are prone to leakage. Thermal conductivity determines the rate of energy storage and release by PCM, which is an important indicator of the performance of PCM applications and one of the bottlenecks existing in the development of phase change energy storage [13,14].

For the problem of PCM leakage, it can be solved by using porous material adsorption or microencapsulation. On the other hand, researchers have attempted to improve the thermal conductivity of PCMs by installing metal fins [15] and adding high thermal conductivity nanoparticles to the PCMs. Some of the thermally conductive fillers that have been developed and used are carbon nanotubes [16], carbon fibers [17], graphene [18], metals [19] and metal oxides [20], and boron nitride [21]. In addition to being

* Corresponding author.
E-mail address: gaochaozibo@163.com (C. Gao).

https://doi.org/10.1016/j.cjche.2024.08.008

inexpensive and simple to use, adding a high thermal conductivity filler to PCM and then using porous material adsorption to create SSPCM is a good way to address the issues of leakage and low thermal conductivity. Mhiri *et al.* [22] prepared paraffin/graphite/carbon foam SSPCM by vacuum impregnation, and the thermal performance test showed that the effective thermal conductivity of this SSPCM was 9 times higher than that of pure PCM, and the melting rate was increased by 42%. Chen *et al.* [23] prepared a composite PCM with good thermal conductivity using paraffin wax as PCM, expanded graphite as adsorbent material, and silicon carbide/silicon dioxide as a high thermal conductivity filler. Mohaisen *et al.* [24] compared the effect of using multi-walled carbon nanotubes as a thermally conductive filler on the thermal conductivity of polyethylene glycol (PEG) for each of the three porous materials, namely, kerosene, pyroxene, and expanded perlite. The results showed that the combination of PEG/EG/multi-walled carbon nanotubes had the best performance, which not only improves the heat storage and release rate but also prevents leakage.

Furthermore, more and more researchers are focusing on inexpensive and renewable bio-based organic PCMs (soybean oil, palm oil, coconut oil, *etc.*), which have better market prospects because they are safer, more environmentally friendly, and more stable [25,26]. However, thermal enhancement studies for these PCMs are still very limited in the published literature.

This work selected coconut oil as PCM due to its suitable phase change temperature and high latent heat, AlN powder with high thermal conductivity was used as a thermally enhanced filler, and EG as a porous adsorbent material. A new SSPCM was prepared using the vacuum impregnation method. Meanwhile, the effect of the content of EG and AlN on the thermophysical properties of composite PCMs was investigated by varying the mass fractions of the three, which were characterized and tested. The results show that the prepared SSPCMs not only have high thermal conductivity but also maintain a high level of thermal storage capacity.

2. Materials and Methods

2.1. Materials

The coconut oil (analytically pure, melting point 20–28 °C, enthalpy of phase change 105 $J \cdot g^{-1}$) was purchased from Shanghai McLean Biochemical Technology Co., Ltd. (China), the expanded graphite (80 mesh, 0.18 mm) was purchased from Qingdao Dongkai Graphite Co., Ltd. (China), and the aluminum nitride (AlN, purity 99%, 10 μm) was supplied by Jiangsu Yuante New Material Technology Co. (China). Before the experiment, the AlN and EG were dried in a vacuum drying oven at 80 °C for 12 h, and all other materials were used directly without treatment.

2.2. Preparation of SSPCM

The SSPCMs were prepared by a simple vacuum impregnation method, and the preparation process is shown in Fig. 1. First, a certain amount of CO was weighed and placed in a beaker in a water bath and heated to 80 °C and maintained for 10 min to melt it completely. Then a certain proportion of AlN powder was added and stirred magnetically for 10 min. Finally, expanded graphite was added and stirred for 2 h. The well-stirred mixture was transferred to a vacuum drying oven and dried at 80 °C and under vacuum for 12 h. After cooling, SSPCM samples were obtained. A portion of the sample was taken and poured into a circular metal mold for pressing before it cooled completely to form a cylindrical sample for leakage testing. Table 1 presents the composition ratios and material nomenclature of the SSPCMs.

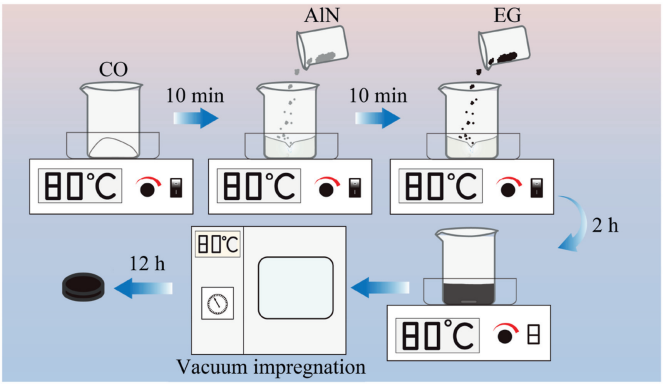

Fig. 1. Preparation process of SSPCMs.

Table 1
Mass content of each component in different SSPCMs

Sample	Mass content/% (mass)		
	CO	EG	AlN
A0E1	90	10	0
A0E1.5	85	15	0
A0E2	80	20	0
A0.5E1	85	10	5
A1E1	80	10	10
A1.5E1	75	10	15
A0.5E1.5	80	15	5

2.3. Characterization

The microstructures of EG, AlN, and SSPCMs were investigated by a scanning electron microscope (SEM, SU-70, Hitachi) at a 10 kV accelerated voltage. X-ray diffractometer (XRD, D8 advance, Bruker, Germany) was used to analyze the chemical characterization of the SSPCMs. The diffraction angle ranged from 10° to 90° at a scan rate of 8 (°)·min^{-1}. The attenuated total reflection-Fourier transform infrared spectra of the samples in the wavelength range of 400–4000 cm^{-1} were obtained using a Fourier transform infrared spectrometer (FT-IR, Nicolet iS50, Thermo Fisher Scientific) and used to analyze the chemical stability of the samples. The thermal stability of SSPCMs was investigated using thermogravimetric experiments conducted on a thermogravimetric analyzer (TGA, STA 449 F5, Netzsch). The material was heated from an initial temperature of 25 °C to 600 °C at a rate of 20 °C· min^{-1} in a nitrogen atmosphere. Differential scanning calorimetry (DSC3, Mettler-Toledo, Sweden) was used to assess the phase change performance of SSPCMs at temperatures ranging from −20 °C to 60 °C, with a temperature rise rate of 5 °C·min^{-1} in a nitrogen (N_2) atmosphere. The thermal conductivity of the prepared SSPCMs was tested with a thermal conductivity tester (TPS2500S from HotDisk), and the thermal conductivity at room temperature (25 °C) was measured using the transient planar heat source method, with the final result being the average of three tests.

3. Results and Discussion

3.1. Morphology and microstructure

Fig. 2 shows the morphology of the pristine and partially composite PCMs. The worm-like EG has dense reticulated micropores Fig. 2(a), which provides for the adsorption of PCMs and thermally conductive particles. AlN particles (Fig. 2(b)) were used as highly thermally conductive materials to enhance heat transfer within CO. In the A0E1 sample (Fig. 2(c)) it can be observed that the voids in

the EG are almost filled with CO and the surface behaves smoother, while in the A0.5E1.5 sample (Fig. 2(d)), It can be seen that the AlN particles are also successfully encapsulated inside the EG and CO. Furthermore, EDS analysis of A0.5E1.5 was performed to obtain the surface elemental distribution. Fig. 2(e) shows the SEM images of selected areas of A0.5E1.5 and the elemental distributions of Al, N, C, and O therein. The elements Al and O are attributed to AlN and CO, respectively. These elements are uniformly distributed, indicating that both AlN and CO are uniformly adsorbed by EG.

Nitrogen adsorption and desorption tests were carried out on the support material EG, and the nitrogen adsorption and desorption curves and BJH pore size distributions of EG are shown in Fig. 3(a) and (b), respectively. The adsorption isotherm is similar to the type IV adsorption isotherm in the classification method published by the International Union of Pure and Applied Chemistry, with monomolecular layer adsorption at lower relative pressures and capillary condensation at higher relative pressures. This indicates the presence of mesoporous (pore size 2–50 nm) structures in EG. In addition, the specific surface area (BET method) of EG reached 124.66 $m^2 \cdot g^{-1}$, which is favorable for the adsorption of CO and AlN particles.

3.2. Crystalline structure

The XRD patterns of the CO, EG, AlN, and SSPCMs are displayed in Fig. 4. EG has a distinct characteristic diffraction peak at $2\theta = 26.6°$. CO has a broad peak at $2\theta = 19.7°$. AlN has typical at $2\theta = 33.2°$ (1 0 0), 36.2° (0 0 2), 38.0° (1 0 1), 49.9° (1 0 2), 59.4° (1 1 0), 66.1° (1 0 3), 69.7° (2 0 0), 71.5° (1 1 2) and 72.6° (2 0 1) diffraction peaks [27]. For composite PCMs, A0E1, A0E1.5, and A0E2 all showed strong peaks of CO and EG at the corresponding positions, whereas A0.5E1, A0.5E1.5, A1E1, and A1.5E1 added the characteristic peaks of AlN. There is no new peak in the XRD pattern

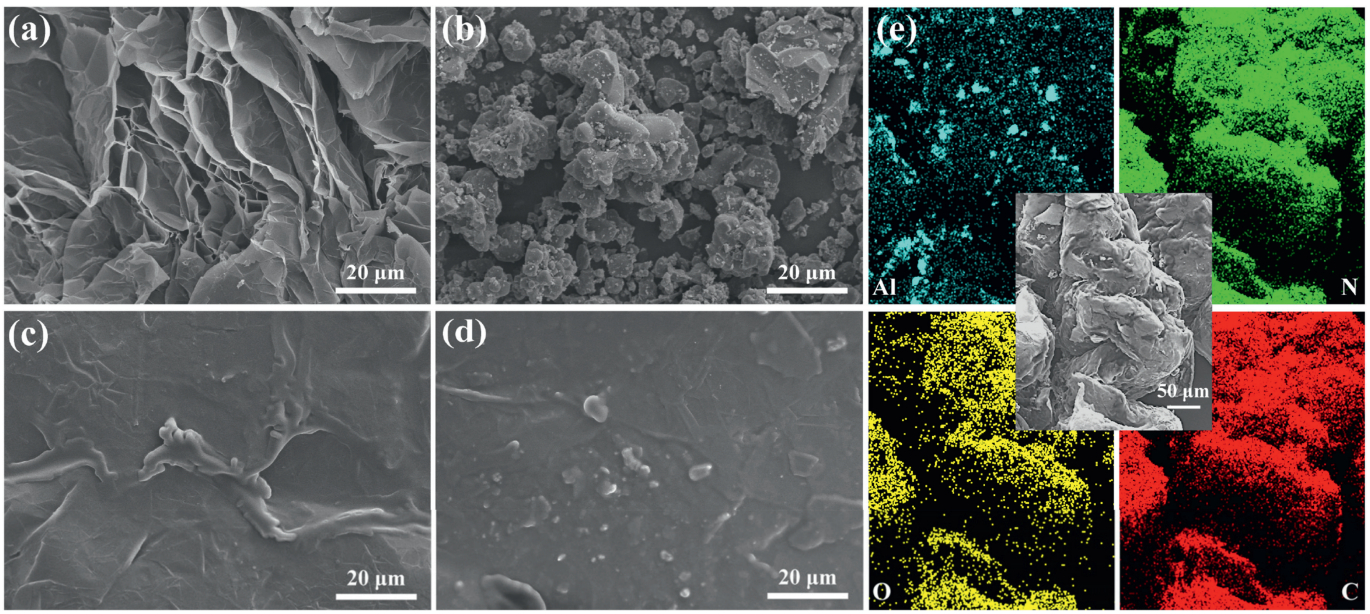

Fig. 2. SEM images of (a) EG, (b) AlN, (c) A0E1, (d) A0.5E1.5. A0.5E1.5 SEM images of selected regions and their EDS images of Al, N, C, and O elements (e).

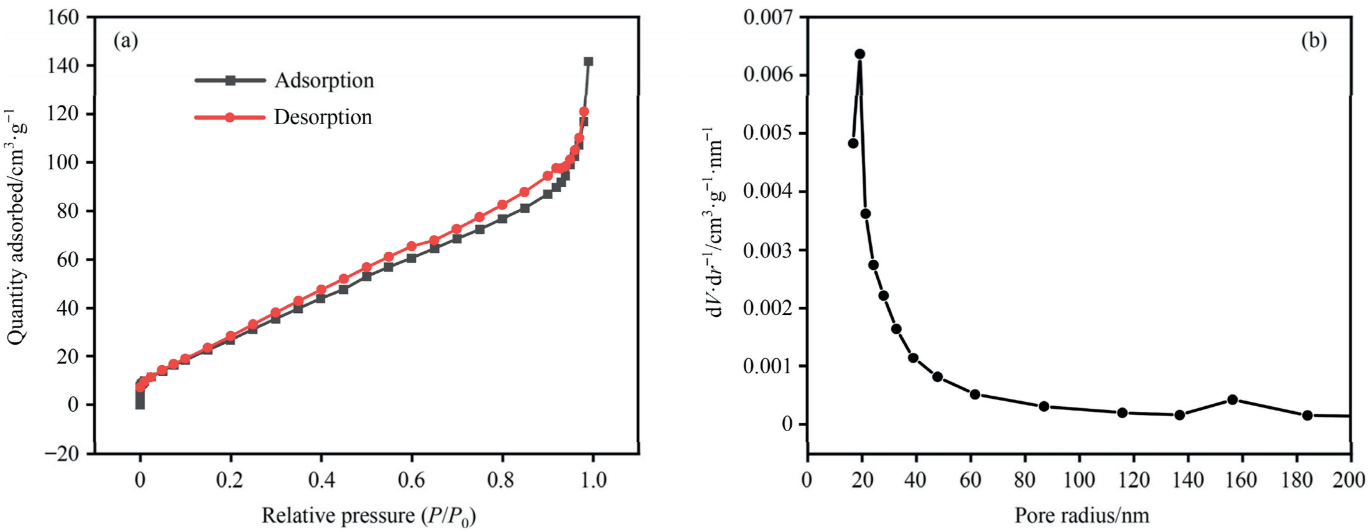

Fig. 3. (a) Nitrogen adsorption isotherm and (b) BJH pore size distribution of EG.

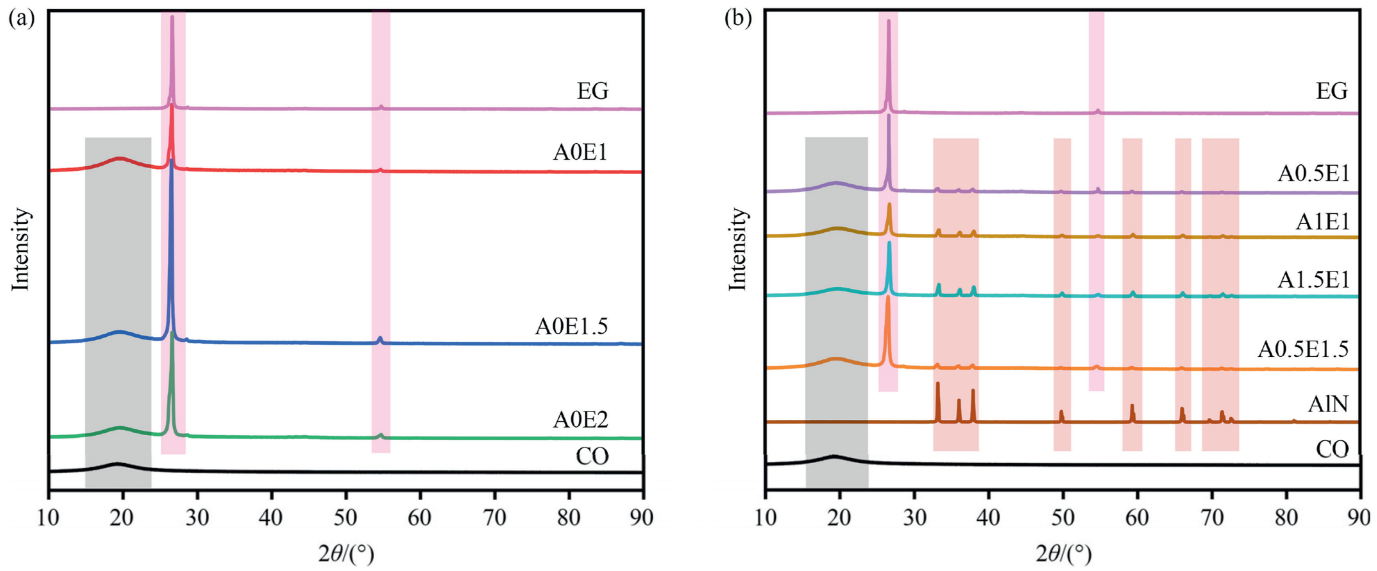

Fig. 4. XRD curves of EG, AlN, CO, and SSPCMs.

of SSPCMs, which indicates that CO, AlN, and EG are physically combined and there is no chemical reaction between them.

3.3. Chemical reliability

ATR-FTIR was used to analyze the interactions between the materials in the composite PCM. The FTIR spectra of CO and SSPCMs prepared in this study are displayed in Fig. 5. The characteristic peaks of CO are mainly sp^3-CH stretching vibration at 2921 cm^{-1} and 2852 cm^{-1}, C═O stretching vibration at 1742 cm^{-1}, sp^3-CH bending vibration at 1465 cm^{-1}, acyl ester C–O vibration at 1154–1112 cm^{-1}, and $-CH_2$ rocking vibration at 721 cm^{-1} [28]. In this experiment, we thoroughly mixed AlN powder with CO and impregnated it into EG. After comparing the Fourier transform infrared (FTIR) peaks of pure CO, CO/EG PCM, and CO/AlN/EG PCM, we found that the characteristic peaks of the SSPCM are merely the superposition of the characteristic peaks of the corresponding constituent materials, and there is no generation of new peaks or disappearance of peaks, except for the difference in peak intensities. This indicates that the materials did not undergo chemical changes during the composite process, and the properties of CO did not change, it can be concluded that the prepared CO/AlN/EG SSPCM has good chemical stability.

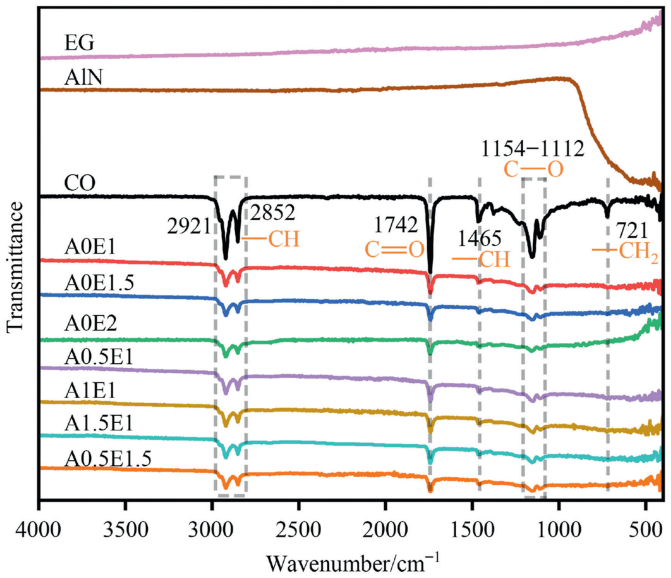

Fig. 5. ATR-FTIR spectra of EG, CO, AlN, and SSPCMs.

3.4. Thermal stability

TGA tests can be used to determine the thermal stability of the new SSPCM by knowing whether intermediate products are generated during the temperature rise process. TGA and derivative thermogravimetric (DTG) curves of pure CO with SSPCM samples are shown in Fig. 6(a) and (b), respectively. The TGA curves show that the mass of all the samples did not change significantly in the temperature range of the phase change of CO. Pure CO does not start to decompose until 285 °C and the decomposition rate reaches a maximum of 429 °C and is almost complete at 500 °C. Interestingly, the onset decomposition temperature of SSPCMs was slightly lower compared to that of pure CO, which may be due to the higher thermal conductivity of SSPCMs, which accelerates the decomposition of SSPCMs [29]. Despite this, the onset decomposition temperature of SSPCMs is still much higher than the melting point of CO (about 23 °C) and its operating temperature. Secondly, all SSPCM samples were degraded in one step and no intermediate substances were generated. The above results indicate that the prepared SSPCMs have good thermal stability. In addition, the weight loss ratio of the SSPCM samples at the end of the test was almost equal to the ratio of CO contained, indicating a good homogeneity of the prepared composites.

3.5. Phase change performance

Fig. 7(a) and (b) show the DSC melting and freezing profiles of pure CO as well as the novel SSPCMs prepared in this study. Their DSC heating and cooling characteristics are shown in Table 2. The melting temperature of CO is 23.09 °C, the freezing temperature is −3.48 °C, and the super-cooling degree is 26.57 °C. As shown in Fig. 7(c), the super-cooling degree of SSPCMs was in the range of 17.73–19.06 °C compared to CO. In Fig. 7, it can be seen the phase change temperature of the PCMs increased slightly after the

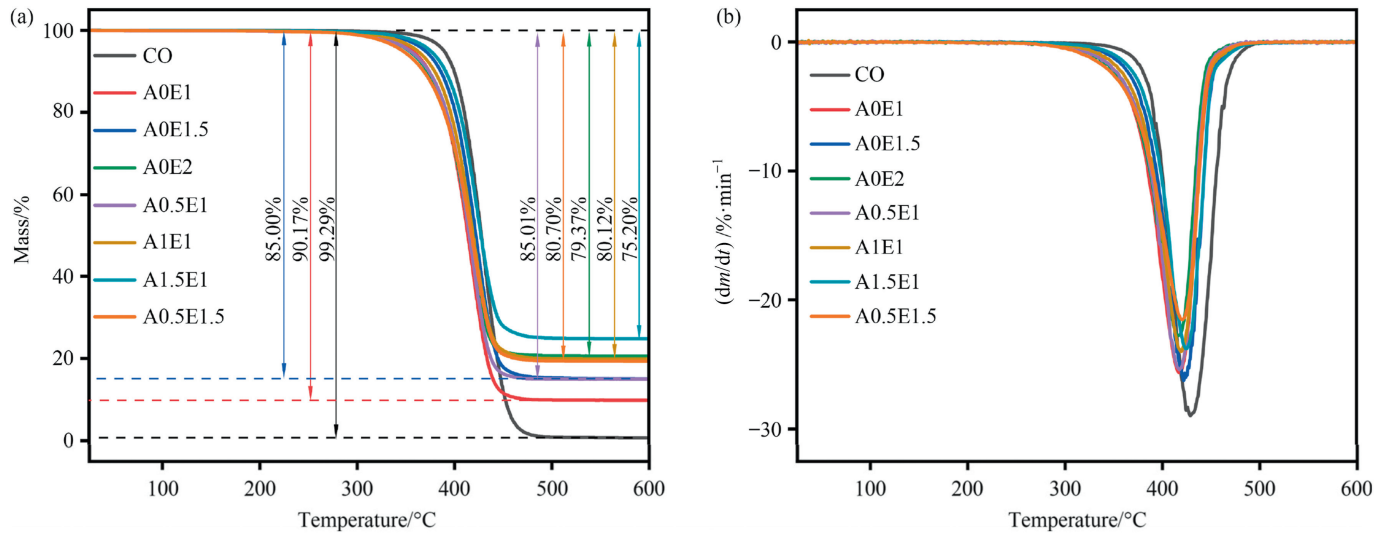

Fig. 6. (a) TGA and (b) DTG curves of CO and SSPCMs.

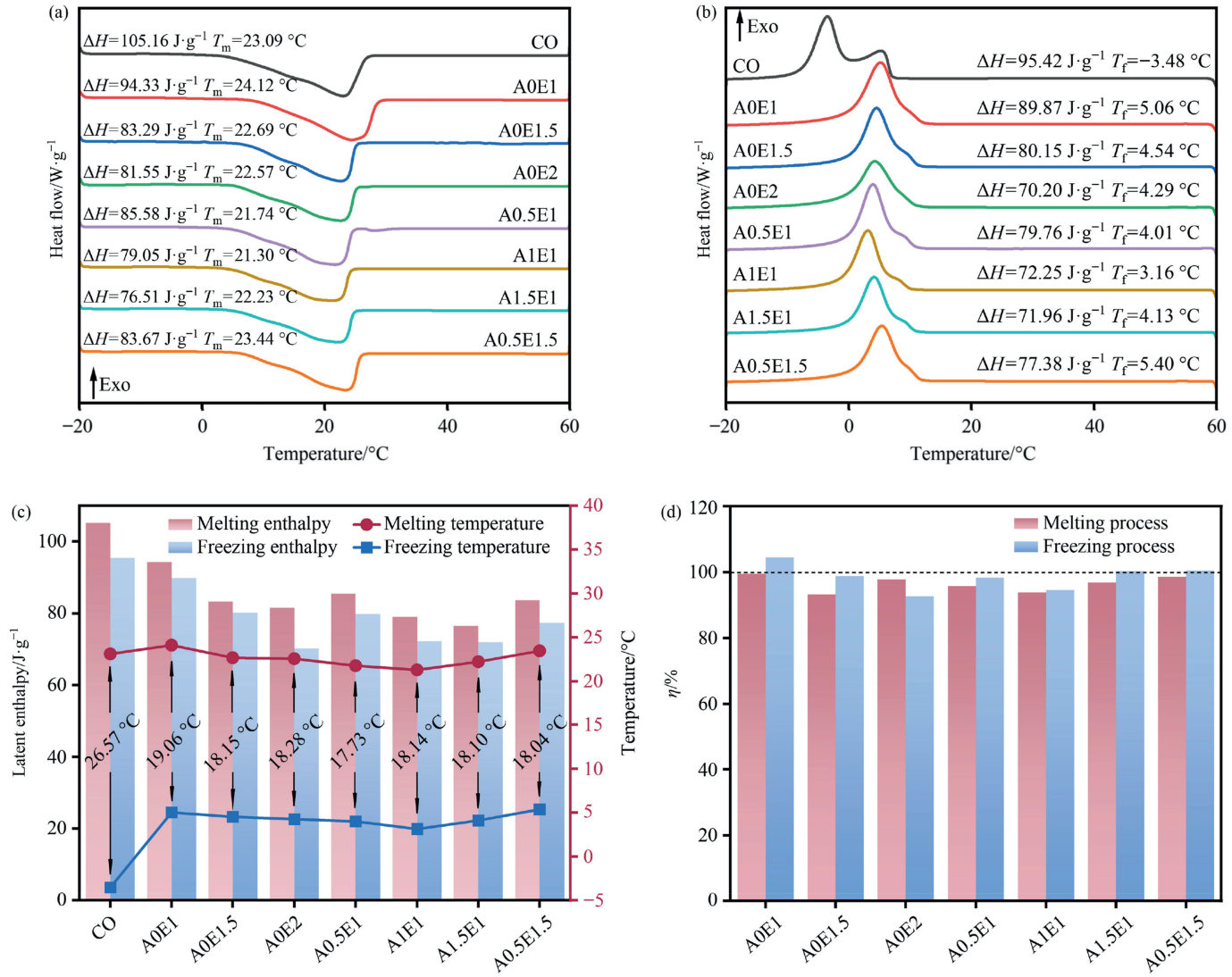

Fig. 7. (a) DSC melting curves and (b) DSC freezing curves of CO and SSPCMs. (c) The phase change temperatures and enthalpies of CO and SSPCMs. (d) The thermal energy storage efficiency of SSPCMs.

Table 2
DSC heating and cooling characteristics of pure CO and SSPCMs

Sample	T_m/°C	ΔH_m/J·g^{-1}	T_f/°C	ΔH_f/J·g^{-1}	Super-cooling degree/°C
CO	23.09	105.16	−3.48	95.42	26.57
A0E1	24.12	94.33	5.06	89.87	19.06
A0E1.5	22.69	83.29	4.54	80.15	18.15
A0E2	22.57	81.55	4.29	70.20	18.28
A0.5E1	21.74	85.58	4.01	79.76	17.73
A1E1	21.30	79.05	3.16	72.25	18.14
A1.5E1	22.23	76.51	4.13	71.96	18.10
A0.5E1.5	23.44	83.67	5.40	77.38	18.04

addition of the supporting material. It may be influenced by the pore characteristics and surface tension [30], and the effect of different supporting materials on the melting temperature of SSPCMs may be different [31,32]. The melting and crystallization temperatures of CO decreased with the increase of EG content, which is likely to be related to the thermal conductivity. The increase in thermal conductivity promotes a more homogeneous phase change process in PCMs [31]. The super-cooling degree of SSPCMs showed a tendency to decrease with increasing mass fraction of EG and AlN, which is attributed to the fact that the added AlN provides heterogeneous nucleation sites for CO, which facilitates the nucleation and crystallization of CO [33]. The DSC curve shows two enthalpy peaks during the solidification process of pure CO, which is similar to a previously reported study [34]. However, due to the addition of EG and AlN, SSPCMs build a good heat conduction network and speed up the heat transfer, so the solidification peak becomes one. In other words, the phase change performance of SSPCMs can be improved by adding EG and AlN. Besides, the latent heat of phase change is one of the most important indexes of PCMs, which will directly affect the heat storage capacity of the materials. The latent heat of melting and freezing of CO is 105.59 J·g^{-1} and 91.38 J·g^{-1}, respectively, which has a very good heat storage capacity. It is worth noting that AlN and EG do not undergo phase change in the tested temperature range, and adding them means that the CO used for heat storage in SSPCMs has to be reduced accordingly, so the enthalpies of phase change of SSPCMs appears to be reduced to some extent. However, the additions of AlN and EG are not too much, so the enthalpies of most of the SSPCMs are still within the acceptable range. In addition, to evaluate the thermal storage capacity of SSPCMs further, the TES efficiency (ŋ) of each sample was calculated by Eq. (1):

$$\eta = \frac{\Delta H_{SSPCMs}}{\Delta H_{CO} \cdot \alpha} \times 100\% \quad (1)$$

where ΔH_{SSPCMs} and ΔH_{CO} denote the enthalpies of phase change of SSPCMs and CO, respectively, and α is the loading amount of CO in SSPCMs obtained in the thermogravimetric test. Fig. 7(d) demonstrates the TES efficiencies of all the SSPCMs, and most of them are above 95%, which means that the SSPCMs maintain a good TES capacity during the preparation process.

3.6. Thermal conductivity

Thermal conductivity is a very critical parameter for SSPCM, good thermal conductivity gives the PCM better heat transfer properties and makes it fulfill the application requirements. The thermal conductivities of CO and SSPCMs are listed in Table 3. From Table 3 and Fig. 8, it can be seen that the thermal conductivity of the SSPCMs can be significantly improved by using the high thermal conductivity of EG and AlN. It is found through the comparative analysis that the effect of EG on the enhancement of thermal conductivity of the composite PCM shows a trend of increasing and then decreasing as the content increases from 10% to 20%. This is probably because 15% of EG has completely absorbed CO. When the content of EG exceeds 15%, the excess pores contain air, which reduces the thermal conductivity. When the EG content is 10%, the addition of 5% AlN reduces the enhancement effect of SSPCM

Table 3
Thermal conductivity and growth rate of SSPCMs

Sample	Thermal conductivity/W·m^{-1}·K^{-1}	Rate of increase/%
CO	0.160	/
A0E1	2.530	1481
A0E1.5	2.125	1228
A0E2	0.684	328
A0.5E1	0.909	468
A1E1	1.799	1024
A1.5E1	2.128	1230
A0.5E1.5	2.985	1765

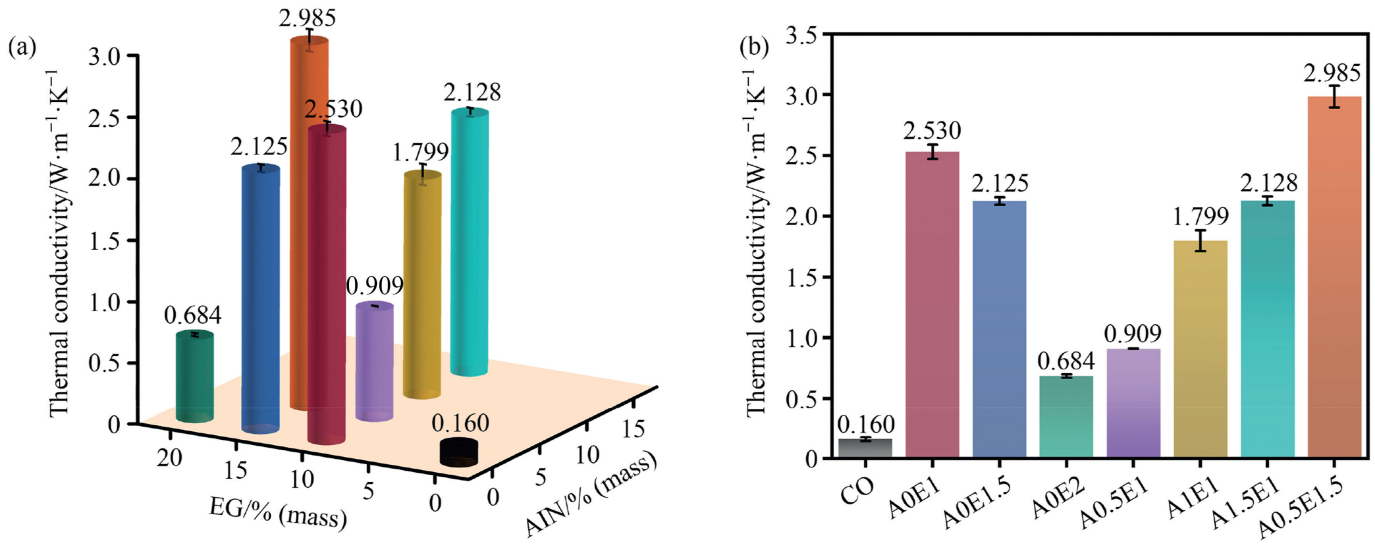

Fig. 8. Effect of mass fraction of EG and AlN on thermal conductivity of SSPCMs.

thermal conductivity, and the enhancement effect increases with the increase of AlN content. This is because at the initial addition of a small amount of AlN nanoparticles, a good thermal conductivity pathway cannot be formed due to the large gaps between particles and particles, and particles and EG. With the increase of AlN content, the gap between particles and EG becomes smaller, the contact thermal resistance decreases, and the enhancement effect of SSPCM thermal conductivity becomes more and more obvious. When the mass fraction of EG and AlN added is 15% and 5% respectively, the thermal conductivity of SSPCM is as high as 2.985 $W \cdot m^{-1} \cdot K^{-1}$, which is 18.65 times that of pure CO. This is because EG has a higher intrinsic thermal conductivity and has a greater impact on thermal conductivity when used as supporting materials than as a thermally conductive filler [35]. However, when the adsorption of CO reaches saturation, further increasing the amount of EG will create voids and reduce the PCM content per unit volume. 15% (mass) EG is just in a critical state, and adding a small amount of AlN makes up for this defect and improves the heat transfer network. This allows EG to maximize its role in enhancing thermal conductivity, and AlN powder also becomes a secondary channel in SSPCM to promote sufficient and uniform heat conduction. In addition, we tried to increase the AlN content based on A0.5E1.5. However, the CO content decreased further, which reduced its bonding ability and aggravated the agglomeration of fillers. Their thermal conductivity also decreased compared with A0.5E1.5. This shows that only when the ratio of EG and AlN is appropriate, their synergistic effect can maximize the improvement of the heat transfer performance of SSPCMs [35].

Table 4 lists some examples of coconut oil-based composite PCMs published in recent years. Comparing the composite PCMs prepared in this study with those prepared in the previous literature in terms of thermal conductivity and thermal storage performance, it can be found that the composite PCMs prepared in this study have both high thermal conductivity and high enthalpy of phase change, and the increase in thermal conductivity does not have too much negative impact on the enthalpy of phase change. The excellent performance suggests that they are suitable for thermal energy storage. Furthermore, by comparing with the first work in Table 4, it is shown that the renewable coconut oil-based SSPCMs proposed in this work have the potential to replace paraffin-based SSPCMs.

3.7. Shape stability

To avoid liquid phase leakage and other undesirable effects after application, PCMs also need to have strong form stability [39]. To evaluate the shape stability of SSPCMs, the samples were placed on a hot table, heated from 15 °C to 80 °C, and maintained for 30 min, and the state of the PCMs before and after heating was recorded using a digital camera. As shown in Fig. 9. Pure CO completely melted and penetrated the whole filter paper after heating. SSPCMs with 10% EG content (A0E1, A0.5E1, A1E1, A1.5E1) had a small amount of liquid leakage after heating. However, SSPCMs (A0E1.5, A0.5E1.5, A0E2) with EG content of 15% and 20% did not leak on the filter paper, which is consistent with our prediction that 15% EG can completely adsorb CO when analyzing the thermal conductivity data. Increasing the EG mass fraction was favorable to improving the shape stability of PCMs. The reason for this phenomenon is that EG has many pores. These pores provide surface tension and capillary forces, which cause the CO to be absorbed into the pores and can effectively prevent its leakage. It is worth noting that the increase of EG decreases the phase change enthalpy of SSPCM accordingly. On the premise of ensuring the shape stability of PCM, the content of EG should be reduced as much as possible. In this experiment, the maximum load of CO in EG is confirmed to be 85%, and it can be considered that the prepared SSPCM has good shape stability in the working temperature range.

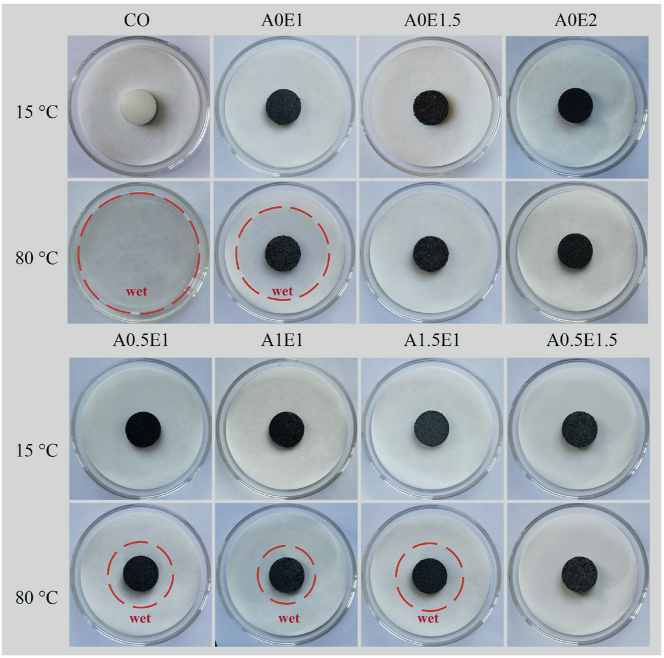

Fig. 9. Shape stability test of SSPCMs.

3.8. Thermal cycle stability

For practical purposes, one of the most crucial parameters for thermal energy storage materials is thermal cycling stability. Therefore, A0.5E1.5, which has mass fractions of 15% for EG and 5% for AlN, was chosen as a representative sample for the thermal cycling experiments in this investigation. Heating A0.5E1.5 from 15 °C to 65 °C and then cooling it from 65 °C to 15 °C completed the cycle 100 times. The DSC curves of A0.5E1.5 after 100 thermal cycles are shown in Fig. 10. Most of the post-cycling DSC curves are similar to the pre-cycling ones, and the subtle difference is the presence of a small peak after the main melting peak (22.98 °C) for A0.5E1.5

Table 4
Comparison of this study with published research

Matrix	Thermally conductive filler	Thermal conductivity/$W \cdot m^{-1} \cdot K^{-1}$	Melting latent heat/$J \cdot g^{-1}$	Ref.
Paraffin	Silicon carbide/expanded graphite	4.086	122.20	[23]
Paraffin	Graphite flakes/epoxy	2.500	104.00	[36]
Paraffin	Copper nanoparticles/diatomite	0.561	95.50	[37]
Coconut oil	Graphene	0.357	102.00	[34]
Coconut oil	Exfoliated graphite nanoplatelets	1.330	82.37	[38]
Coconut oil	Activated carbon	0.460	43.80	[31]
Coconut oil	Aluminum nitride/expanded graphite	2.985	83.67	This work

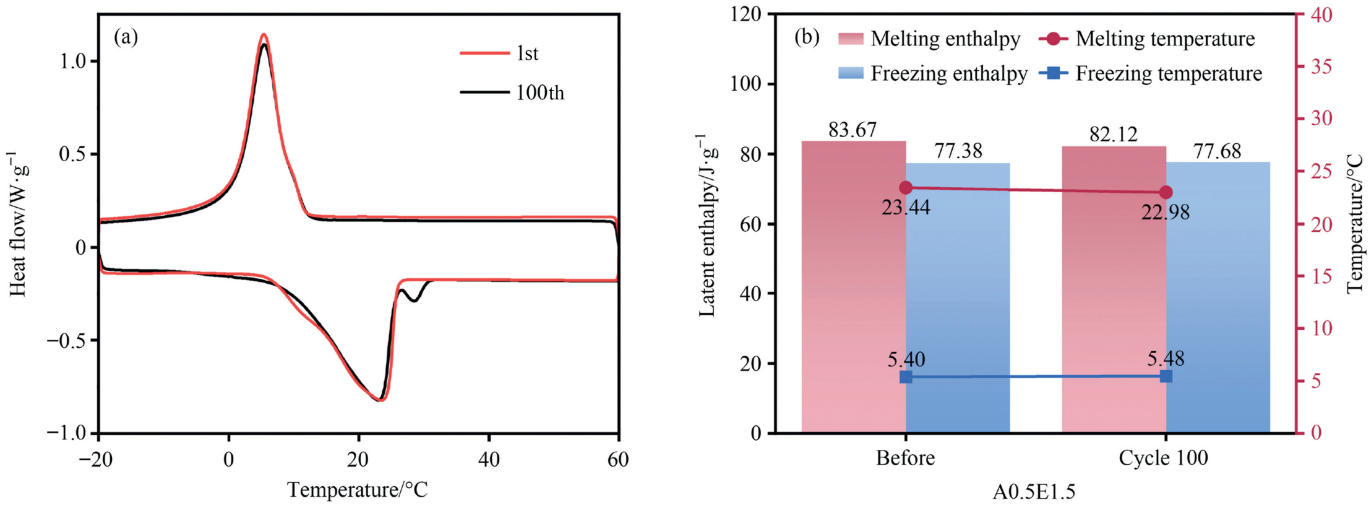

Fig. 10. DSC curve of the A0.5E1.5 after 1 and 100 thermal cycles.

after cycling. This may be the result of the small number of defective crystals that appeared in CO after multiple cycles due to the limitation of the support material EG, which led to the melting and recrystallization during the heating process [40]. Nevertheless, the enthalpy of melting of A0.5E1.5 decreased only slightly from 83.67 $J \cdot g^{-1}$ to 82.12 $J \cdot g^{-1}$, with an enthalpy loss of 1.8%, and the melting peak decreased from 23.44 °C to 22.98 °C. The above results show that the prepared SSPCM still has good thermal storage properties after many reuses.

4. Conclusions

In this work, SSPCMs were prepared by vacuum impregnation method using coconut oil as PCM, AlN as thermally conductive enhancement particles, and EG as structural support material. The results showed that both AlN and EG significantly enhanced the thermal conductivity of the SSPCMs with a synergistic enhancement effect. The greatest enhancement in thermal conductivity of SSPCM was achieved when the mass fractions of coconut oil, aluminum nitride, and expanded graphite were 80%, 5%, and 15%, respectively, and reached 2.985 $W \cdot m^{-1} \cdot K^{-1}$, which is 1765% higher compared to pure coconut oil. Furthermore, DSC analysis showed that the melting point of A0.5E1.5 was almost indistinguishable from that of coconut oil with a latent heat value of 83.67 $J \cdot g^{-1}$. The FTIR, XRD, and TGA results indicated good thermal and chemical stability of the prepared SSPCMs. In addition, thermal cycle tests show that after 100 thermal cycles, the melting enthalpy of A0.5E1.5 decreases by 1.8%, and the phase change temperature remains unchanged. The good thermophysical properties make it suitable for thermal energy storage.

Declaration of Competing Interest

The authors declare that they have no known competing financial interests or personal relationships that could have appeared to influence the work reported in this paper.

CRediT Authorship Contribution Statement

Chao Gao: Writing – review & editing, Writing – original draft, Supervision, Project administration, Methodology, Funding acquisition, Data curation, Conceptualization. Feng Jiang: Writing – original draft, Investigation, Formal analysis, Data curation. Benguo Zhang: Supervision, Resources. Mingchuan Shen: Validation, Investigation. Yuguo Zhang: Resources, Investigation.

Acknowledgements

We sincerely thank Soochow University for providing us with some of the resources needed to conduct this survey.

References

[1] D. Lefebvre, F.H. Tezel, A review of energy storage technologies with a focus on adsorption thermal energy storage processes for heating applications, *Renew. Sustain. Energy Rev.* 67 (2017) 116–125.
[2] Y. Ahmadi, K.H. Kim, S. Kim, M. Tabatabaei, Recent advances in polyurethanes as efficient media for thermal energy storage, *Energy Storage Mater.* 30 (2020) 74–86.
[3] C.N. Zou, F. Ma, S.Q. Pan, Q. Zhao, G.Y. Fu, G.S. Zhang, Y.C. Yang, H. Yu, Y.B. Liang, M.J. Lin, Y. Wang, B. Xiong, H.L. Liu, Global energy transition revolution and the connotation and pathway of the green and intelligent energy system, *Petrol. Explor. Dev.* 50 (3) (2023) 722–740.
[4] A. Hussain, S.M. Arif, M. Aslam, Emerging renewable and sustainable energy technologies: state of the art, *Renew. Sustain. Energy Rev.* 71 (2017) 12–28.
[5] M. Waterson, The characteristics of electricity storage, renewables and markets, *Energy Pol.* 104 (2017) 466–473.
[6] X.B. Huang, X. Chen, A. Li, D. Atinafu, H.Y. Gao, W.J. Dong, G. Wang, Shape-stabilized phase change materials based on porous supports for thermal energy storage applications, *Chem. Eng. J.* 356 (2019) 641–661.
[7] K. Pielichowska, K. Pielichowski, Phase change materials for thermal energy storage, *Prog. Mater. Sci.* 65 (2014) 67–123.
[8] H.Q. Liu, K.Y. Sun, X.Y. Shi, H.N. Yang, H.S. Dong, Y. Kou, P. Das, Z.S. Wu, Q. Shi, Two-dimensional materials and their derivatives for high performance phase change materials: emerging trends and challenges, *Energy Storage Mater.* 42 (2021) 845–870.
[9] S. Gong, X.L. Li, M.J. Sheng, S. Liu, Y.F. Zheng, H. Wu, X. Lu, J.P. Qu, High thermal conductivity and mechanical strength phase change composite with double supporting skeletons for industrial waste heat recovery, *ACS Appl. Mater. Interfaces* 13 (39) (2021) 47174–47184.
[10] J. Luo, D.Q. Zou, Y.S. Wang, S. Wang, L. Huang, Battery thermal management systems (BTMs) based on phase change material (PCM): a comprehensive review, *Chem. Eng. J.* 430 (2022) 132741.
[11] M.F. Junaid, Z.U. Rehman, N. Ijaz, M. Čekon, J. Čurpek, A. Babeker Elhag, Bio-based phase change materials from a perspective of recycling, resources conservation and green buildings, *Energy Build.* 270 (2022) 112280.
[12] R. Kalbasi, Usefulness of PCM in building applications focusing on envelope heat exchange–Energy saving considering two scenarios, *Sustain. Energy Technol. Assess.* 50 (2022) 101848.
[13] D.L. Feng, Y.Y. Zang, P. Li, Y.H. Feng, Y.Y. Yan, X.X. Zhang, Polyethylene glycol phase change material embedded in a hierarchical porous carbon with superior thermal storage capacity and excellent stability, *Compos. Sci. Technol.* 210 (2021) 108832.
[14] Y.L. Li, T. Zou, J. Zhao, T. Zhang, P.Y. Deng, W.W. Liu, X.G. Zhang, C.J. Xie, High-enthalpy aramid nanofiber aerogel-based composite phase change materials with enhanced thermal conductivity, *Compos. Commun.* 40 (2023) 101614.

[15] A. Mostafavi, M. Parhizi, A. Jain, Theoretical modeling and optimization of fin-based enhancement of heat transfer into a phase change material, *Int. J. Heat Mass Transf.* 145 (2019) 118698.
[16] R.I. Rabady, D.S. Malkawi, Thermal conductivity enhancement of sodium thiosulfate pentahydrate by adding carbon nano-tubes/graphite nano-particles, *J. Energy Storage* 27 (2020) 101166.
[17] Y.N. Liu, N.N. Wang, Y.F. Ding, Preparation and properties of composite phase change material based on solar heat storage system, *J. Energy Storage* 40 (2021) 102805.
[18] O. Ola, Y. Chen, Y.Q. Zhu, Three-dimensional carbon foam nanocomposites for thermal energy storage, *Sol. Energy Mater. Sol. Cells* 191 (2019) 297–305.
[19] R.L. Wen, S.B. Zhu, M.M. Wu, W.X. Chen, Design and preparation of Ag modified expanded graphite based composite phase change materials with enhanced thermal conductivity and light-to-thermal properties, *J. Energy Storage* 41 (2021) 102936.
[20] I. Daou, L. El-Kaddadi, O. Zegaoui, M. Asbik, N. Zari, Structural, morphological and thermal properties of novel hybrid-microencapsulated phase change materials based on Fe_2O_3, ZnO and TiO_2 nanoparticles for latent heat thermal energy storage applications, *J. Energy Storage* 17 (2018) 84–92.
[21] J.H. Zhou, G.H. Du, J.F. Hu, X. Lai, S. Liu, Z.G. Zhang, The establishment of Boron nitride@sodium alginate foam/polyethyleneglycol composite phase change materials with high thermal conductivity, shape stability, and reusability, *Chin. J. Chem. Eng.* 54 (2023) 11–21.
[22] H. Mhiri, A. Jemni, H. Sammouda, Numerical and experimental investigations of melting process of composite material (nanoPCM/carbon foam) used for thermal energy storage, *J. Energy Storage* 29 (2020) 101167.
[23] M.Y. Chen, S.Y. Zhang, L.Y. Zhao, J.W. Weng, D.X. Ouyang, Q.P. Chen, Q.H. Kong, J. Wang, Preparation of thermally conductive composite phase change materials and its application in lithium-ion batteries thermal management, *J. Energy Storage* 52 (2022) 104857.
[24] K.O. Mohaisen, M. Hasan Zahir, M. Maslehuddin, S.U. Al-Dulaijan, Development of a shape-stabilized phase change material utilizing natural and industrial byproducts for thermal energy storage in buildings, *J. Energy Storage* 50 (2022) 104205.
[25] C. Baylis, C.A. Cruickshank, Review of bio-based phase change materials as passive thermal storage in buildings, *Renew. Sustain. Energy Rev.* 186 (2023) 113690.
[26] R.K. Mishra, K. Verma, V. Mishra, B. Chaudhary, A review on carbon-based phase change materials for thermal energy storage, *J. Energy Storage* 50 (2022) 104166.
[27] X.H. Chen, K.E. Gonsalves, Synthesis and properties of an aluminum nitride/polyimide nanocomposite prepared by a nonaqueous suspension process, *J. Mater. Res.* 12 (5) (1997) 1274–1286.
[28] J. Jeon, J.H. Park, S. Wi, S. Yang, Y.S. Ok, S. Kim, Latent heat storage biocomposites of phase change material-biochar as feasible eco-friendly building materials, *Environ. Res.* 172 (2019) 637–648.
[29] J. Yang, E.W. Zhang, X.F. Li, Y.T. Zhang, J. Qu, Z.Z. Yu, Cellulose/graphene aerogel supported phase change composites with high thermal conductivity and good shape stability for thermal energy storage, *Carbon* 98 (2016) 50–57.
[30] D.G. Atinafu, B.Y. Yun, S. Wi, Y. Kang, S. Kim, A comparative analysis of biochar, activated carbon, expanded graphite, and multi-walled carbon nanotubes with respect to PCM loading and energy-storage capacities, *Environ. Res.* 195 (2021) 110853.
[31] A.R. Muchtar, C.L. Hassam, B. Srinivasan, D. Berthebaud, T. Mori, N. Soelami, B. Yuliarto, Shape-stabilized phase change materials: performance of simple physical blending synthesis and the potential of coconut based materials, *J. Energy Storage* 52 (2022) 104974.
[32] B.E. Jebasingh, Exfoliation of graphite by solar irradiation and investigate their thermal property on capric–myristic–palmitic acid/exfoliated graphite composite as phase change material (PCM) for energy storage, *J. Energy Storage* 5 (2016) 70–76.
[33] T. Zhang, T.D. Zhang, J. Zhang, D.Y. Zhang, P.R. Guo, H.X. Li, C.L. Li, Y. Wang, Design of stearic acid/graphene oxide-attapulgite aerogel shape-stabilized phase change materials with excellent thermophysical properties, *Renew. Energy* 165 (2021) 504–513.
[34] L. Safira, N. Putra, T. Trisnadewi, E. Kusrini, T.M.I. Mahlia, Thermal properties of sonicated graphene in coconut oil as a phase change material for energy storage in building applications, *Int. J. Low Carbon Technol.* 15 (4) (2020) 629–636.
[35] Y. Wang, J.F. Hu, Z.M. Zhu, G.H. Du, X. Lai, Z.G. Zhang, Assembling and characterizing of high-loading and steady-shape graphene aerogel composite phase change material with nano-AlN–as an efficient thermal conductivity enhancer, *Sol. Energy Mater. Sol. Cells* 249 (2023) 112041.
[36] A. Ohayon-Lavi, A. Lavi, A. Alatawna, E. Ruse, G. Ziskind, O. Regev, Graphite-based shape-stabilized composites for phase change material applications, *Renew. Energy* 167 (2021) 580–590.
[37] D.J. Wu, X.B. Gu, Q. Sun, W.M. Luo, B.B. Zhang, J.G. Peng, L. Bian, K.J. Dong, Thermal conductivity enhancement of diatomite-based composite phase change materials by interfacial reduction deposition of Cu nanoparticles, *J. Energy Storage* 61 (2023) 106861.
[38] S. Wi, J. Seo, S.G. Jeong, S.J. Chang, Y.J. Kang, S. Kim, Thermal properties of shape-stabilized phase change materials using fatty acid ester and exfoliated graphite nanoplatelets for saving energy in buildings, *Sol. Energy Mater. Sol. Cells* 143 (2015) 168–173.
[39] T.Y. Wang, S.F. Wang, R.L. Luo, C.Y. Zhu, T. Akiyama, Z.G. Zhang, Microencapsulation of phase change materials with binary cores and calcium carbonate shell for thermal energy storage, *Appl. Energy* 171 (2016) 113–119.
[40] Y. Qian, P. Wei, P.K. Jiang, Z. Li, Y.G. Yan, J.P. Liu, Preparation of a novel PEG composite with halogen-free flame retardant supporting matrix for thermal energy storage application, *Appl. Energy* 106 (2013) 321–327.